Quaternary International 464 (2018) 364–369

Contents lists available at ScienceDirect

Quaternary International

journal homepage: www.elsevier.com/locate/quaint

Microcodium in Chinese loess as a recorder for the oxygen isotopic composition of monsoonal rainwater

Zeke Zhang [a, b, c, *], Gaojun Li [b], Hong Yan [a], Zhisheng An [a]

[a] State Key Lab of Loess and Quaternary Geology, Institute of Earth Environment, Chinese Academy of Sciences, Xi'an 710061, China
[b] MOE Key Laboratory of Surficial Geochemistry, Department of Earth Sciences, Nanjing University, 163 Xianlindadao, Nanjing 210023, China
[c] University of Chinese Academy of Sciences, Beijing 100049, China

ARTICLE INFO

Article history:
Received 25 August 2017
Received in revised form
24 October 2017
Accepted 31 October 2017
Available online 14 November 2017

Keywords:
Chinese Loess Plateau
Climate change
Paleosol
East Asia monsoon
Precipitation $\delta^{18}O$

ABSTRACT

Records of Asia Summer Monsoon (ASM) from the Chinese loess and the speleothem display distinct features. The very different proxies that were applied to the two archives may be responsible for this discrepancy. A direct comparison between the speleothem and the loess records under the same proxy system of rainwater $\delta^{18}O$ may help to resolve this puzzle. Here we show that the calcified microcodium in the loess deposits may record the oxygen isotopic composition of the summer rainwater. A microcodium based $\delta^{18}O$ record covering the past 140 kyrs was generated, which shows similar magnitude of the overall variation to that of the speleothem records. However, much weaker precession variability was registered in the microcodium record during the last interglacial period. Instead, the microcodium $\delta^{18}O$ record is more consistent with the widely used summer monsoon proxy of magnetic susceptibility in the loess deposits with clear glacial-interglacial pattern. This similarity may originate from the low sedimentation rate of the interglacial paleosol layer that preferentially record the peak ASM signals on the precession band. It is also possible that the orbital variability of ASM between the North China and South China is inherently different with more ice-volume related influence in the north. A longer microcodium $\delta^{18}O$ record in sequences of higher sedimentation rate and a reliable record of summer rainfall may help to resolve these possibilities.

1. Introduction

The dominant orbital cycles of summer precipitation, which is of great importance to decipher the driving force of monsoonal climate, have been found to be very different in region influenced by ASM (An et al., 2011, 2015; Bloemendal et al., 1995; Cai et al., 2015; Cheng et al., 2016; Clemens et al., 2010; Kathayat et al., 2016; Li et al., 2017; Nie et al., 2008, 2017; Sun et al., 2006; Wang et al., 2014). On the northern margin of the ASM influenced region, the records based on the loess-and-paleosol sequences from the Chinese Loess Plateau (CLP) display a coexistence of 100-, 41-, and 23-kyr periods with dominance of 100-kyr cycles after the mid-Pleistocene transition (Ding et al., 1995; Kukla et al., 1990; Liu, 1985; Liu et al., 1999; Sun et al., 2015). However, the speleothem stable oxygen isotopic records from the southern China reveal dominance of precession cycles (23-kyr) (Cheng et al., 2009, 2016; Wang et al., 2008; Yuan et al., 2004). This complexity may originate from the very different proxies applied to the two archives as the processes, besides the strength of ASM, that affect the proxy value, may be very different. Comparing the records of loess and speleothem under the same proxy system may have the potential to clarify this puzzle.

Oxygen isotope of rainwater is a widely used hydrological tracer for the intensity of ASM due to the preferential removal of heavy ^{18}O isotope from water vapor during condensation of cloud droplet (Dansgaard, 1964; Hu et al., 2008; Yuan et al., 2004). It is generally accepted that stronger ASM produces more negative $\delta^{18}O$ value of rainwater. Cave deposits in widespread regions across the East and South Asia show coherent variation of $\delta^{18}O$ (Cheng et al., 2016) that is consistent with the anticipated influence of precession and North Atlantic cooling on the intensity of ASM on orbital (Kutzbach, 1981) and millennial time scale (Lin et al., 2013, 2014, 2017; Wang et al., 2001), respectively. Following the same reason, the $\delta^{18}O$ value of rainwater on the CLP may also record the strength of ASM because the CLP is located on the northern margin of ASM influenced region

* Corresponding author. State Key Lab of Loess and Quaternary Geology, Institute of Earth Environment, Chinese Academy of Sciences, Xi'an 710061, China.
E-mail address: zhangzk@ieecas.cn (Z. Zhang).

https://doi.org/10.1016/j.quaint.2017.10.050
1040-6182/

so that the accumulative effect of precipitation in East Asia can be reflected.

Chinese loess is a typical calcareous soil (Liu, 1985) that contains abundant carbonate minerals for the $\delta^{18}O$ researches. It has been shown that the carbonate in loess is a mixture of pedogenic carbonate and detrital carbonate (Li et al., 2013). Thus, investigations on the oxygen isotopic composition of carbonate in the loess deposits are challenging and very limited (Chen et al., 1996; Han et al., 1997; Li et al., 2007; Sheng et al., 2002). Among these limited studies, most of the $\delta^{18}O$ records were generated from the carbonate nodules (Ding and Yang, 2000; Ji et al., 2017; Rao et al., 2006; Suarez et al., 2011) although other types authigenic carbonates are also abundant in the loess deposits. The best carbonate record of rainwater $\delta^{18}O$ should have a quasi-continuous distribution and a purely authigenic origin. However, the formation of carbonate nodules is related to the re-deposition of the leached carbonate in its overlying soil layer. Both of the leaching and the re-deposition require distinct climate conditions. A wet condition is needed for leaching while a much too wet condition may inhibit carbonate re-deposition. Thus, the distribution of carbonate nodule in the loess deposits is rather scattered with concentrated abundance at the bottom of paleosol layers (An et al., 1989). Evidences from trace metal compositions (Li et al., 2013) and intra-specimen variations of $\delta^{13}C$ and $\delta^{18}O$ (Yang et al., 2012) also suggest existence of significant amount of detrital carbonate in the carbonate nodule. The precipitation season of the carbonate nodule is also unclear while only the $\delta^{18}O$ of summer rainfall can reflect the strength of ASM. Thus, a continuously distributed pure authigenic carbonate that precipitates during the summer season is desired to reconstruct the $\delta^{18}O$ of monsoonal rainwater and thus the strength of ASM.

Recent works have shown that microcodium, a calcified plant debris, is rather continuously distributed in the loess deposits (Li et al., 2017). Trace element compositions of the microcodium show a purely authigenic origin with little detrital contamination (Li and Li, 2014). It has been shown that the microcodium can record the trace element composition of soil water that was controlled by summer monsoon intensity (Li and Li, 2014; Li et al., 2017). Thus, the microcodium in the loess deposits has great potential to record the $\delta^{18}O$ of monsoonal precipitation.

This work investigates the suitability of microcodium in Chinese loess as a recorder for the $\delta^{18}O$ of monsoonal rainwater. The $\delta^{18}O$ values of the modern and Holocene microcodium are used to constrain the seasonality of the microcodium records. A microcodium $\delta^{18}O$ record is generated on the central CLP covering the last interglacial-glacial cycles. The paleoclimate implication of the new record is also discussed associated with other summer monsoon proxies in the loess and cave deposits.

2. Material and methods

Holocene paleosol were collected from ten sites across the CLP (Fig. 1). The modern soil developed on the eolian deposits of late Holocene was also collected from Weinan site (109°29′E, 34°27′N) to the south margin of CLP. Samples of eolian deposits covering the past 140 kyrs were collected at 5-cm (~500 yr) resolution from the Xifeng section (107°47′E, 35°45′N) on the central CLP. Magnetic susceptibility (MS) of the samples was measured at low-frequency using Bartington Instrument MS2B meter to establish stratigraphy of the sections.

Different types of authigenic carbonate, namely microcodium, carbonate nodule, matrix carbonate, rhizoconcretion, and strawberry-like carbonate grains were picked from the sieved sediment (>75 μm) by hand under binocular microscope. For most of the samples, about twenty pieces of microcodium were picked to reduce the intra-sample variability. The picked carbonate of every sample was then crashed and mixed in a vial. The oxygen isotopic compositions of the mixed carbonate were analyzed by a MAT-253

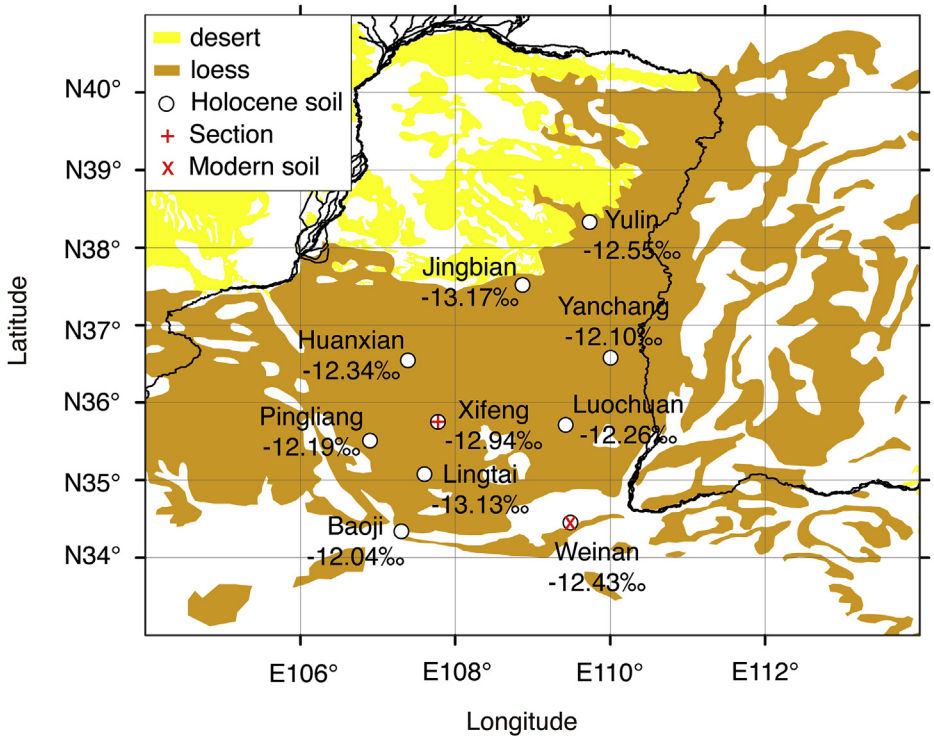

Fig. 1. Map showing the sampling sites on the CLP. The $\delta^{18}O$ values of microcodium from the Holocene paleosol across the CLP are also labeled.

Table 1
$\delta^{18}O$ values (‰, PDB) of individual microcodium pieces within one sample.

$\delta^{18}O$ (1)	$\delta^{18}O$ (2)	$\delta^{18}O$ (3)	$\delta^{18}O$ (4)	Mean	σ_s
−15.75	−14.10	−14.64	−14.77	−14.82	0.69

gas sourced mass spectrometry using a Kiel IV carbonate device at the Nanjing Institute of Geology and Palaeontology, Chinese Academy of Sciences (CAS). Standard isotopic corrections were applied and the oxygen-isotope compositions were reported in $\delta^{18}O$ relative to PDB. The precision of the carbonate standard samples is 0.08‰ in standard derivation for $\delta^{18}O$. Standard deviation (σ_s) of $\delta^{18}O$ among individual microcodium pieces within one sample is about 0.69‰ (Table 1), which may reflect inter-annual variations. Thus, the average $\delta^{18}O$ uncertainty measured on homogenized microcodium of 20 pieces is estimated to be about 0.15‰ ($\sigma_m = \sigma_s/\sqrt{n}$, $n = 20$).

The age model of the magnetic susceptibility record of the Xifeng Section is established by the accepted correlation (Ding et al., 2002; Hao et al., 2012; Sun et al., 2006) between the grain size (Sun et al., 2006), which reflects the strength of winter monsoon, and the global ice volume (Lisiecki and Raymo, 2005). The rapid shifts in the grain size that correspond to the glacial terminations is used as tie points of the age model. Between tie points, grain-size weighted interpolation is used (Porter and Zhisheng, 1995). To avoid possible downward leaching effect of the microcodium record, the age model of the microcodium $\delta^{18}O$ record is constructed by tying the rapid shift of $\delta^{18}O$ during the marine isotope stages (MIS) 6/5, 5/4, 2/1 transitions to the speleothem records.

3. Results

The $\delta^{18}O$ values of different types of authigenic carbonates picked from the Holocene paleosol show large variation (Table 2). The $\delta^{18}O$ values of microcodium are much lower than those of the other types of authigenic carbonates by about 2–4‰. The $\delta^{18}O$ value of modern microcodium from Weinan is characterized by a narrow range with a very low average value of −11.2‰ ± 0.5‰ (2σ, n = 5) (Table 3). Holocene paleosol across the CLP also show narrow range and even slightly lower $\delta^{18}O$ values of microcodium from −12.04‰ to −13.17‰ (Fig. 1). The $\delta^{18}O$ values of Holocene microcodium show no correlation with the local climate factors, such as summer temperature and precipitation amount (Fig. 2). No strong positive correlation can be found between the $\delta^{13}C$ and $\delta^{18}O$ value of microcodium from Xifeng profile ($r^2 = 0.09$).

The $\delta^{18}O$ values of microcodium from the Xifeng section vary from −10‰ to −16‰ (Fig. 3a). Similar low $\delta^{18}O$ values are observed in MIS 1, 3, 5 and similar high $\delta^{18}O$ values appear in MIS 2, 4, 6 (Fig. 3).

Table 2
$\delta^{18}O$ values (‰, PDB) of different carbonates picked from Holocene samples within one sample.

Carbonate	Pingliang	Huanxian	Yanchang
Microcodium	−12.87	−12.34	−12.10
Carbonate nodule	−9.19	−8.51	−8.16
Matrix carbonate	−10.32	−8.62	−9.41
Rhizoconcretion	−9.91	−10.74	−10.13
Strawberry-like carbonate grain	−10.59	–	–

Table 3
$\delta^{18}O$ values (‰, PDB) of modern microcodium from Weinan.

$\delta^{18}O$ (1)	$\delta^{18}O$ (2)	$\delta^{18}O$ (3)	$\delta^{18}O$ (4)	$\delta^{18}O$ (5)	Mean	σ_s
−11.11	−11.52	−11.34	−10.84	−11.32	−11.23	0.26

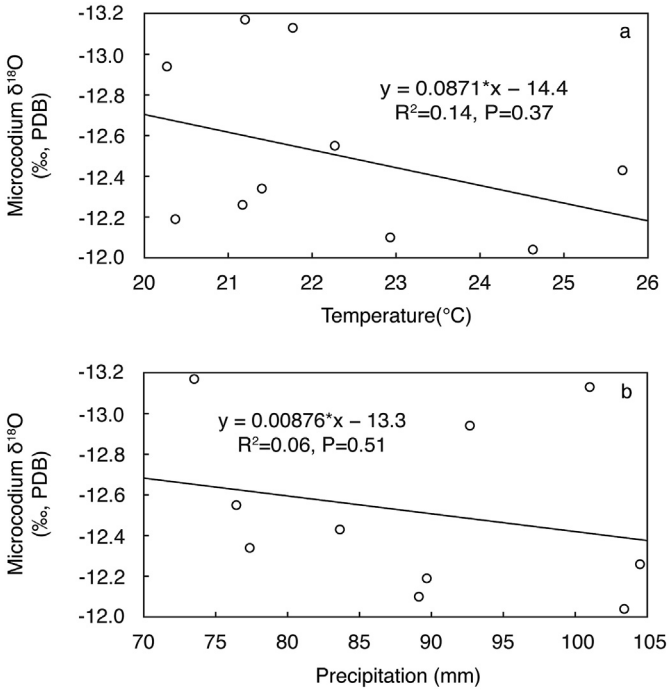

Fig. 2. Correlation between the microcodium $\delta^{18}O$ of Holocene paleosol across the CLP and summer (June-July-August) monthly mean temperature (a), and summer monthly mean precipitation (b). Temperature and precipitation data are derived from China Meteorological Data Sharing Service System.

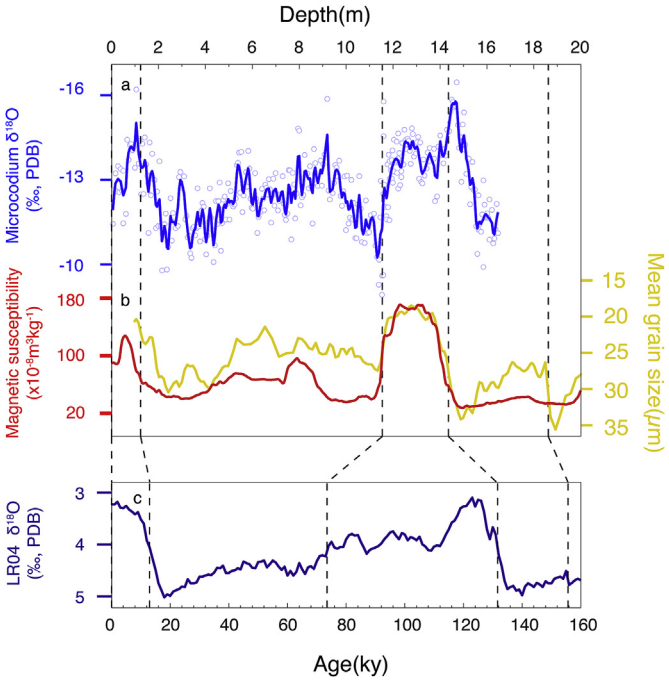

Fig. 3. The microcodium $\delta^{18}O$ record in Xifeng section and age model. (a) Microcodium $\delta^{18}O$ record plotted on depth scale (smoothed by a 5-cm width Gaussian filter). (b) Mean grain size of quartz (yellow)(Sun et al., 2006) and MS (red) plotted on depth scale. (c) LR04 composite of benthic $\delta^{18}O$ (Laskar et al., 2004). Vertical dash lines show the tie points of the age model. (For interpretation of the references to colour in this figure legend, the reader is referred to the web version of this article.)

4. Discussion

4.1. Formation season of microcodium

The very low $\delta^{18}O$ value of microcodium compared with other types of authigenic carbonates (Table 1) can be explained by the combination of a summer formation of the microcodium and a minimum influence of transpiration on the soil water $\delta^{18}O$. The lack of positive correlations between $\delta^{13}C$ and $\delta^{18}O$ suggest limited effect of kinetic fractionation (Hendy, 1971; Wang et al., 2001). Thus, the formation season of microcodium can be traced by comparing the $\delta^{18}O$ value of modern microcodium to that of the expected authigenic carbonate precipitated in different monthly based on the observed rainwater $\delta^{18}O$ and the equilibrium fractionation factor determined by soil temperature. The monthly average $\delta^{18}O$ of rainwater in the studied region has been well constrained by International Atomic Energy Agency (Fig. 4a). The equilibrium fractionation factor between calcite and water is based on Kim and O'Neil (1997):

$$1000 \ln \alpha = 18.03 \times 10^3/T - 32.42$$

where α is the fractionation factor, T is the soil temperature in Kelvin at 0.05 m depth (Fig. 4b). The expected $\delta^{18}O$ of the calcite precipitated during summer show the lowest value due to the combined effects of low rainwater $\delta^{18}O$ and high temperature.

The $\delta^{18}O$ value of modern microcodium from Weinan, a site near Xi'an where the monthly GNIP $\delta^{18}O$ data is available, only matches with that of calcite precipitated during summer season (Fig. 4c).

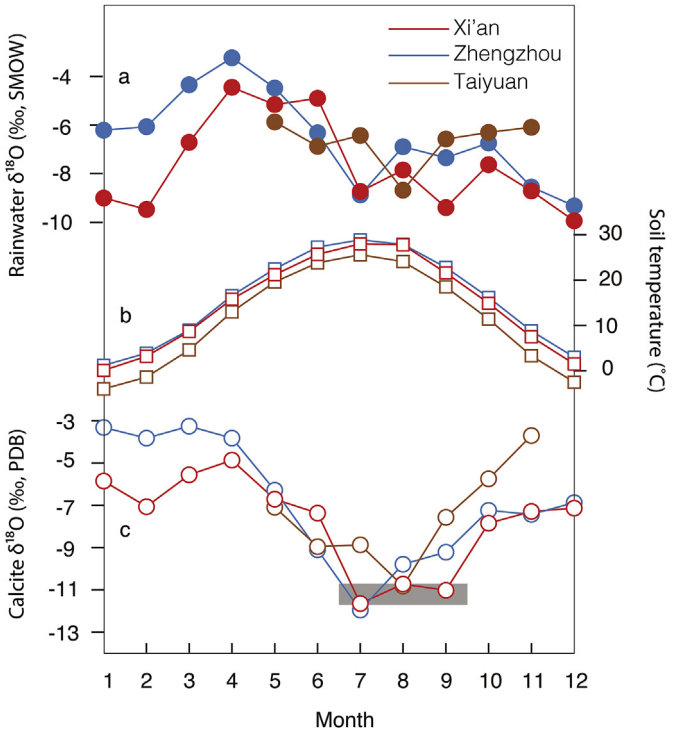

Fig. 4. The expected $\delta^{18}O$ of calcite precipitated during different seasons. (a) Oxygen isotopic composition of rainwater around CLP. The data is derived from the Global Network of Isotopes in Precipitation (GNIP) database from their web site at http://www-naweb.iaea.org/napc/ih/IHS_resources_gnip.html. The stations with good data (more than 2 calendar year) around CLP are used. (b) Monthly mean surface soil temperature at 0.05 m depth. Temperature data are derived from China Meteorological Data Sharing Service System. (c) Calculated oxygen isotopic composition of calcite. The grey bar shows the range of modern microcodium $\delta^{18}O$.

Possible deeper depth of microcodium formation and thus lower summer soil temperature compared to the surface soil temperature may result in higher expected $\delta^{18}O$ value of the calcite precipitation. The possible influence of transpiration will also result in higher $\delta^{18}O$ value of soil solution and thus the authigenic calcite. Thus, the match of modern microcodium to the lowest expected $\delta^{18}O$ value of the authigenic calcite argues strongly a summer formation of microcodium and a minimum effect of transpiration on the soil $\delta^{18}O$. A summer precipitation of microcodium is consistent with the suggestion of summer time formation of soil carbonate according to the clumped isotope thermometry (Quade et al., 2013).

4.2. Influence of temperature

The effect of temperature on the equilibrium isotope fractionation should be considered when using the $\delta^{18}O$ of microcodium to reflect that of the rainwater. The temperature dependence of oxygen isotope fractionation between calcite and water is about ~-0.23‰/°C (Kim and O'Neil, 1997). Such a low temperature sensitivity may help to explain the lack of correlation between temperature and the microcodium $\delta^{18}O$ for the Holocene soil across the CLP (Fig. 2) because temperature changes of less than 6 °C could only introduce $\delta^{18}O$ variation of less than 1.38‰ while the influence of other variability such as regional changes of rainwater $\delta^{18}O$ may largely exceed this value.

The influence of temperature on the microcodium $\delta^{18}O$ is also limited on glacial-interglacial scale. The assumed maximum 8 °C difference between glacial and interglacial periods (Braconnot et al., 2007; Eagle et al., 2013) on the CLP would only lead to a variation about 1.84‰, which is much smaller than the observation of ~6‰. Thus, being similar to the speleothem $\delta^{18}O$ (Cheng et al., 2006), microcodium $\delta^{18}O$, may mainly reflect the changes of rainwater $\delta^{18}O$.

4.3. Paleoclimate implications

Similarity between the microcodium $\delta^{18}O$ and the speleothem $\delta^{18}O$ records can be found (Fig. 5). The ~6‰ overall variation of the microcodium $\delta^{18}O$ is similar to that of Chinese speleothem (Cheng et al., 2016). Being similar to the speleothem $\delta^{18}O$ record, the microcodium $\delta^{18}O$ record also shows similar value during MIS 3 comparable to those during the MIS 1 and MIS 5.

The major difference between the microcodium $\delta^{18}O$ and speleothem $\delta^{18}O$ is during the MIS 5 where precession cycles are much weaker/absent in microcodium record (Fig. 5). The lack of procession cycles during the MIS 5 results in consistence between the microcodium $\delta^{18}O$ and the widely used summer monsoon proxy of magnetic susceptibility (An et al., 1991; Liu et al., 2012; Maher, 2016; Nie, 2011; Zhou et al., 1990) in the loess deposits with clear ice-volume related pattern. The major discrepancy between the microcodium $\delta^{18}O$ and magnetic susceptibility is the signal amplitude during the MIS 3. It has been argued that a lower magnetic susceptibility value during the MIS 3 compared to those during MIS I and 5 may reflect influence of higher sedimentation rate on the accumulation of pedogenic magnetic enhancement because the ^{10}Be flux show similar precipitation amount of the MIS 3 compared to those of MIS 1 and 5 (Zhou et al., 2014).

The lack of precession cycles of the microcodium $\delta^{18}O$ record during the MIS 5 may originate from the low sedimentation rate of the interglacial paleosol layer that may preferentially record the peak ASM signals on the precession band. It is also possible that the orbital variations of ASM between the North China and the South China are inherently different with more ice-volume related influence in the north. It has been suggested that the speleothem $\delta^{18}O$ may largely reflect processes such as the upper stream rainfall in

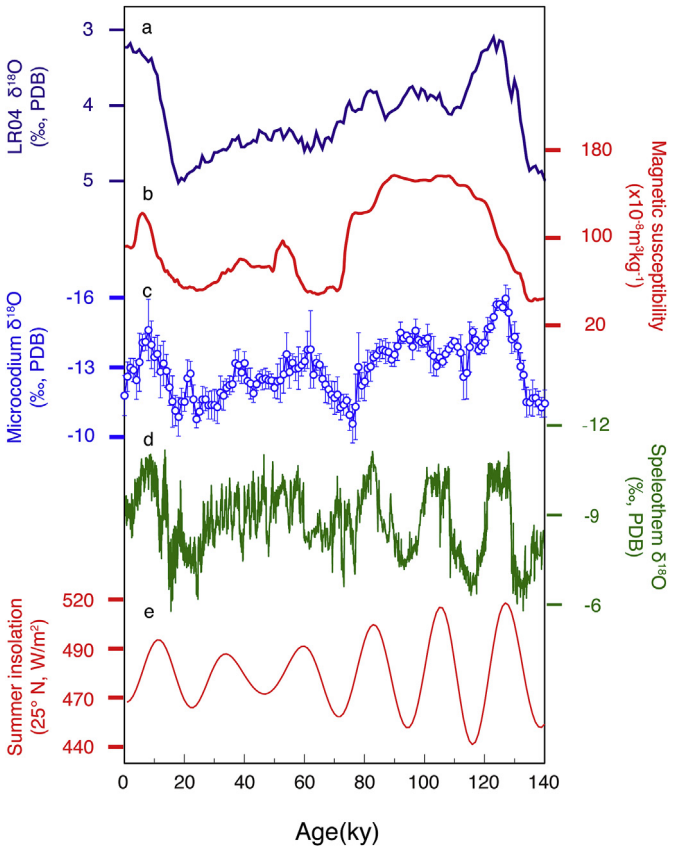

Fig. 5. Comparing the microcodium $\delta^{18}O$ record with other time series. (a) LR04 composite of deep seawater $\delta^{18}O$ that reflects global ice volume (Lisiecki and Raymo, 2005). (b) The loess magnetic susceptibility. (c) The stacked microcodium $\delta^{18}O$ with error bar showing 2× standard error of the stacked mean (open cycles are smoothed record using a 0.5-ky Gaussian filter). (d) Speleothem $\delta^{18}O$ (Cheng et al., 2016). (e) The summer (June 21st) insolation at 25° N.

tropics rather than the strength of ASM. Thus, we argue that the similarity between the microcodium $\delta^{18}O$ and speleothem $\delta^{18}O$ records may originate from the inherited $\delta^{18}O$ signal of south China while the difference between the microcodium $\delta^{18}O$ and speleothem $\delta^{18}O$ records indicates that the strength of ASM may have experienced influence of ice-volume related factors such as temperature, pCO_2 (Lu et al., 2013), and land to sea distances (Ding et al., 1995; Liu and Ding, 1998).

5. Conclusion

Constrains based on the $\delta^{18}O$ of modern precipitation and soil temperature indicate that the very low $\delta^{18}O$ value of the calcified microcodium in Chinese loess is caused by the summer time precipitation of the calcite crystals. Being benefited from limited influence of transpiration and crystallization temperature, the $\delta^{18}O$ of microcodium can reflect that of summer rainwater. The $\delta^{18}O$ of summer rainfall recorded by the microcodium shows a pattern that is more similar to the glacial-interglacial pattern of the widely used monsoon proxy of magnetic susceptibility in the loess deposits rather than the precession dominated speleothem $\delta^{18}O$ records in the South China. Lower deposition rate of loess during the interglacial period and thus possible homogenization of the precession signal due to the pedogenic turnover may contribute partly to the difference between the microcodium and speleothem records. It is also very likely that the strength of ASM in East Asia is very different from the tropical monsoon that generates the speleothem $\delta^{18}O$ signals though upper stream depletion. A longer microcodium $\delta^{18}O$ record in profiles with higher deposition rate may help to clarify the discrepancy between the loess and the speleothem records in future.

Acknowledgements

This study was supported by the Chinese Academy of Sciences (QYZDY-SSW-DQC001) and the National Natural Science Foundation of China (no. 41420104008, 41422205, and 41730101).

References

An, Z., Clemens, S.C., Ji, S., Qiang, X., Jin, Z., Sun, Y., Prell, W.L., Luo, J., Wang, S., Xu, H., 2011. Glacial-interglacial Indian summer monsoon dynamics. Science 333, 719–723.
An, Z., Kukla, G., Liu, T., 1989. Loess stratigraphy in luochuan of China. Quat. Sci. 9, 155–168.
An, Z., Kukla, G.J., Porter, S.C., Xiao, J., 1991. Magnetic susceptibility evidence of monsoon variation on the Loess Plateau of central China during the last 130,000 years. Quat. Res. 36, 29–36.
An, Z., Wu, G., Li, J., Sun, Y., Liu, Y., Zhou, W., Cai, Y., Duan, A., Li, L., Mao, J., 2015. Global monsoon dynamics and climate change. Annu. Rev. Earth Planet. Sci. 43, 2.1-2.49.
Bloemendal, J., Liu, X.M., Rolph, T.C., 1995. Correlation of the magnetic susceptibility stratigraphy of Chinese loess and the marine oxygen isotope record: chronological and palaeoclimatic implications. Earth Planet. Sci. Lett. 131, 371–380.
Braconnot, P., Ottobliesner, B., Kageyama, M., Kitoh, A., Loutre, M.F., Marti, O., Merkel, U., Ramstein, G., Valdes, P., Weber, S.L., 2007. Results of PMIP2 Coupled Simulations of the Mid-holocene and Last Glacial Maximum - Part 1 : Experiments and Large-scale Features. Copernicus Gmbh.
Cai, Y., Fung, I.Y., Edwards, R.L., An, Z., Cheng, H., Lee, J.-E., Tan, L., Shen, C.-C., Wang, X., Day, J.A., 2015. Variability of stalagmite-inferred Indian monsoon precipitation over the past 252,000 y. Proc. Natl. Acad. Sci. 112, 2954–2959.
Chen, J., An, Z., Wang, H., Gao, Y., 1996. An isotopic study of the S1 paleosol carbonates from the central Loess Plateau of North China. Chin. Sci. Bull. 41, 1542–1545.
Cheng, H., Edwards, R.L., Broecker, W.S., Denton, G.H., Kong, X., Wang, Y., Zhang, R., Wang, X., 2009. Ice age terminations. Science 326, 248–252.
Cheng, H., Edwards, R.L., Sinha, A., Spötl, C., Yi, L., Chen, S., Kelly, M., Kathayat, G., Wang, X., Li, X., Kong, X., Wang, Y., Ning, Y., Zhang, H., 2016. The Asian monsoon over the past 640,000 years and ice age terminations. Nature 534, 640–646.
Cheng, H., Edwards, R.L., Wang, Y., Kong, X., Ming, Y., Kelly, M.J., Wang, X., Gallup, C.D., Liu, W., 2006. A penultimate glacial monsoon record from Hulu Cave and two-phase glacial terminations. Geology 34, 217–220.
Clemens, S.C., Prell, W.L., Sun, Y., 2010. Orbital-scale timing and mechanisms driving Late Pleistocene Indo-Asian summer monsoons: reinterpreting cave speleothem δ18O. Paleoceanography 25.
Dansgaard, W., 1964. Stable isotopes in precipitation. Tellus 16, 436–468.
Ding, Z., Liu, T., Rutter, N.W., Yu, Z., Guo, Z., Zhu, R., 1995. Ice-volume forcing of East Asian winter monsoon variations in the past 800,000 years. Quat. Res. 44, 149–159.
Ding, Z.L., Derbyshire, E., Yang, S.L., Yu, Z.W., Xiong, S.F., Liu, T.S., 2002. Stacked 2.6-Ma grain size record from the Chinese loess based on five sections and correlation with the deep-sea δ18O record. Paleoceanography 17, 5–1-5-21.
Ding, Z.L., Yang, S.L., 2000. C3/C4 vegetation evolution over the last 7.0 Myr in the Chinese Loess Plateau: evidence from pedogenic carbonate δ13C. Palaeogeogr. Palaeoclimatol. Palaeoecol. 160, 291–299.
Eagle, R.A., Risi, C., Mitchell, J.L., Eiler, J.M., Seibt, U., Neelin, J.D., Li, G., Tripati, A.K., 2013. High regional climate sensitivity over continental China constrained by glacial-recent changes in temperature and the hydrological cycle. Proc. Natl. Acad. Sci. 110, 8813–8818.
Han, J., Keppens, E., Liu, T., Paepe, R., Jiang, W., 1997. Stable isotope composition of the carbonate concretion in loess and climate change. Quat. Int. 37, 37–43.
Hao, Q., Wang, L., Oldfield, F., Peng, S., Qin, L., Song, Y., Xu, B., Qiao, Y., Bloemendal, J., Guo, Z., 2012. Delayed build-up of Arctic ice sheets during 400,000-year minima in insolation variability. Nature 490, 393–396.
Hendy, C.H., 1971. The isotopic geochemistry of speleothems—I. The calculation of the effects of different modes of formation on the isotopic composition of speleothems and their applicability as palaeoclimatic indicators. Geochim. Cosmochim. Acta 35, 801–824.
Hu, C., Henderson, G.M., Huang, J., Xie, S., Sun, Y., Johnson, K.R., 2008. Quantification of Holocene Asian monsoon rainfall from spatially separated cave records. Earth Planet. Sci. Lett. 266, 221–232.
Ji, S., Nie, J., Breecker, D.O., Luo, Z., Song, Y., 2017. Intensified aridity in northern China during the middle Piacenzian warm period. J. Asian Earth Sci. 147, 222–225.
Kathayat, G., Cheng, H., Sinha, A., Spötl, C., Edwards, R.L., Zhang, H., Li, X., Yi, L., Ning, Y., Cai, Y., Lui, W.L., Breitenbach, S.F.M., 2016. Indian monsoon variability on millennial-orbital timescales. Sci. Rep. 6, 24374.
Kim, S.-T., O'Neil, J.R., 1997. Equilibrium and nonequilibrium oxygen isotope effects

in synthetic carbonates. Geochim. Cosmochim. Acta 61, 3461–3475.
Kukla, G., An, Z.S., Melice, J.L., Gavin, J., Xiao, J.L., 1990. Magnetic susceptibility record of Chinese loess. Trans R. Soc. Edn. Earth Sci. Trans. R. Soc. Edinb. Earth Sci. 81, 263–288.
Kutzbach, J.E., 1981. Monsoon climate of the early Holocene: climate experiment with the earth's orbital parameters for 9000 years ago. Science 214, 59–61.
Laskar, J., Robutel, P., Joutel, F., Gastineau, M., Correia, A.C.M., Levrard, B., 2004. A long-term numerical solution for the insolation quantities of the Earth. Astron. Astrophys. 428, 261–285.
Li, G., Chen, J., Chen, Y., 2013. Primary and secondary carbonate in Chinese loess discriminated by trace element composition. Geochim. Cosmochim. Acta 103, 26–35.
Li, G.J., Sheng, X.F., Chen, J., Yang, J.D., Chen, Y., 2007. Oxygen-isotope record of paleorainwater in authigenic carbonates of Chinese loess-paleosol sequences and its paleoclimatic significance. Palaeogeogr. Palaeoclimatol. Palaeoecol. 245, 551–559.
Li, T., Li, G., 2014. Incorporation of trace metals into microcodium as novel proxies for paleo-precipitation. Earth Planet. Sci. Lett. 386, 34–40.
Li, T., Liu, F., Abels, H.A., You, C.-F., Zhang, Z., Chen, J., Ji, J., Li, L., Li, L., Liu, H.-C., Ren, C., Xia, R., Zhao, L., Zhang, W., Li, G., 2017. Continued obliquity pacing of East Asian summer precipitation after the mid-Pleistocene transition. Earth Planet. Sci. Lett. 457, 181–190.
Lin, D.-C., Chen, M.-T., Yamamoto, M., Yokoyama, Y., 2013. Precisely dated AMS 14C marine cores reveal the complexity of millennial-scale Asian monsoon variability in the northern South China Sea (MD972146, MD972148). J. Asian Earth Sci. 69, 93–101.
Lin, D.-C., Chen, M.-T., Yamamoto, M., Yokoyama, Y., 2014. Millennial-scale alkenone sea surface temperature changes in the northern South China Sea during the past 45,000 years (MD972146). Quat. Int. 333, 207–215.
Lin, D.-C., Chen, M.-T., Yamamoto, M., Yokoyama, Y., 2017. Hydrographic variability in the northern South China Sea over the past 45,000 years: new insights based on temperature reconstructions by UK'37 and TEXH86 proxies from a marine sediment core (MD972146). Quat. Int. 459, 1–16.
Lisiecki, L.E., Raymo, M.E., 2005. A Pliocene-Pleistocene stack of 57 globally distributed benthic δ 18 O records. Paleoceanography 20, 1–16.
Liu, D., 1985. Loess and Environment in China. Science Press, Beijing (in Chinese).
Liu, Q., Roberts, A.P., Larrasoaña, J.C., Banerjee, S.K., Guyodo, Y., Tauxe, L., Oldfield, F., 2012. Environmental magnetism: principles and applications. Rev. Geophys. 50, 197–215.
Liu, T., Ding, Z., 1998. Chinese loess and the paleomonsoon. Annu. Rev. Earth Planet. Sci. 26, 111–145.
Liu, T., Ding, Z., Rutter, N., 1999. Comparison of Milankovitch periods between continental loess and deep sea records over the last 2.5 Ma. Quat. Sci. Rev. 18, 1205–1212.
Lu, H., Yi, S., Liu, Z., Mason, J.A., Jiang, D., Cheng, J., Stevens, T., Xu, Z., Zhang, E., Jin, L., 2013. Variation of East Asian monsoon precipitation during the past 21 k.y. and potential CO2 forcing. Geology 41, 1023–1026.
Maher, B.A., 2016. Palaeoclimatic records of the loess/palaeosol sequences of the Chinese Loess Plateau. Quat. Sci. Rev. 154, 23–84.
Nie, J., 2011. Coupled 100-kyr cycles between 3 and 1 Ma in terrestrial and marine paleoclimatic records. Geochem. Geophys. Geosystems 12, 1241–1249.
Nie, J., Garzione, C., Su, Q., Liu, Q., Rui, Z., Heslop, D., Necula, C., Zhang, S., Song, Y., Zeng, L., 2017. Dominant 100,000-year precipitation cyclicity in a late Miocene lake from northeast Tibet. Sci. Adv. 3, e1600762.
Nie, J., King, J.W., Fang, X., 2008. Tibetan uplift intensified the 400 k.y. signal in paleoclimate records at 4 Ma. Geol. Soc. Am. Bull. 120, 1338–1344.
Porter, S.C., Zhisheng, A., 1995. Correlation between Climate Events in the North Atlantic and China during the Last Glaciation.
Quade, J., Eiler, J., Daeron, M., Achyuthan, H., 2013. The clumped isotope geothermometer in soil and paleosol carbonate. Geochim. Cosmochim. Acta 105, 92–107.
Rao, Z., Zhu, Z., Chen, F., Zhang, J., 2006. Does δ13Ccarb of the Chinese loess indicate past C3/C4 abundance? A review of research on stable carbon isotopes of the Chinese loess. Quat. Sci. Rev. 25, 2251–2257.
Sheng, X.F., Chen, J., Yang, J.D., Ji, J.F., Chen, Y., 2002. Carbon and oxygen isotopic composition of carbonate in different grain fractions from loess-paleosol sequences, China. Geochimica 31, 105–112.
Suarez, M.B., Passey, B.H., Kaakinen, A., 2011. Paleosol carbonate multiple isotopologue signature of active East Asian summer monsoons during the late Miocene and Pliocene. Geology 39, 1151–1154.
Sun, Y., Clemens, S.C., An, Z., Yu, Z., 2006. Astronomical timescale and palaeoclimatic implication of stacked 3.6-Myr monsoon records from the Chinese Loess Plateau. Quat. Sci. Rev. 25, 33–48.
Sun, Y., Kutzbach, J., An, Z., Clemens, S., Liu, Z., Liu, W., Liu, X., Shi, Z., Zheng, W., Liang, L., 2015. Astronomical and glacial forcing of East Asian summer monsoon variability. Quat. Sci. Rev. 115, 132–142.
Wang, P.X., Wang, B., Cheng, H., Fasullo, J., Guo, Z.T., Kiefer, T., Liu, Z.Y., 2014. The global monsoon across timescales: coherent variability of regional monsoons. Clim. Past 10, 2007–2052.
Wang, Y., Cheng, H., Edwards, R.L., Kong, X., Shao, X., Chen, S., Wu, J., Jiang, X., Wang, X., An, Z., 2008. Millennial-and orbital-scale changes in the East Asian monsoon over the past 224,000 years. Nature 451, 1090–1093.
Wang, Y.-J., Cheng, H., Edwards, R.L., An, Z.S., Wu, J.Y., Shen, C.C., Dorale, J.A., 2001. A high-resolution absolute-dated late Pleistocene monsoon record from Hulu Cave, China. Science 294, 2345–2348.
Yang, S., Ding, Z., Wang, X., Tang, Z., Gu, Z., 2012. Negative δ 18 O–δ 13 C relationship of pedogenic carbonate from northern China indicates a strong response of C 3/C 4 biomass to the seasonality of Asian monsoon precipitation. Palaeogeogr. Palaeoclimatol. Palaeoecol. 317, 32–40.
Yuan, D., Cheng, H., Edwards, R.L., Dykoski, C.A., Kelly, M.J., Zhang, M., Qing, J., Lin, Y., Wang, Y., Wu, J., 2004. Timing, duration, and transitions of the last interglacial Asian monsoon. Science 304, 575–578.
Zhou, L.P., Oldfield, F., Wintle, A.G., Robinson, S.G., Wang, J.T., 1990. Partly pedogenic origin of magnetic variations in Chinese loess. Nature 346, 737–739.
Zhou, W., Xian, F., Du, Y., Kong, X., Wu, Z., 2014. The last 130 ka precipitation reconstruction from Chinese loess 10Be. J. Geophys. Res. 119, 191–197.